Journal of Cardiovascular Magnetic Resonance 26 (2024) 101102

Contents lists available at ScienceDirect

Journal of Cardiovascular Magnetic Resonance

journal homepage: www.sciencedirect.com/journal/jocmr

Original Research

Assessment of abnormal transvalvular flow and wall shear stress direction for pediatric/young adults with bicuspid aortic valve: A cross-sectional four-dimensional flow study

Takashi Fujiwara[a,*,1], LaDonna J. Malone[a], Kathryn C. Chatfield[b], Alex Berthusen[a,2], Brian Fonseca[c], Lorna P. Browne[a], Alex J. Barker[a,d]

[a] Department of Radiology, Section of Pediatric Radiology, Children's Hospital Colorado, University of Colorado Anschutz Medical Campus, 13123 E 16th Ave, Aurora, Colorado 80045, USA
[b] Department of Pediatrics, Division of Cardiology, University of Colorado Anschutz Medical Campus, Children's Hospital Colorado, 13123 E 16th Ave, Aurora, Colorado 80045, USA
[c] Department of Pediatrics, Section of Pediatric Cardiology, Children's Hospital Colorado, University of Colorado Anschutz Medical Campus, 13123 E 16th Ave, Aurora, Colorado 80045, USA
[d] Department of Bioengineering, University of Colorado Anschutz Medical Campus, 12705 E Montview Blvd, Aurora, Colorado 80045, USA

ARTICLE INFO

Keywords:
Bicuspid aortic valve
4D flow MRI
Pediatrics
Congenital heart disease
Aortic dilation

ABSTRACT

Background: Aortic dilation is seen in pediatric/young adult patients with bicuspid aortic valve (BAV), and hemodynamic markers to predict aortic dilation are necessary for monitoring. Although promising hemodynamic metrics, such as abnormal wall shear stress (WSS) magnitude, have been proposed for adult BAV patients using four-dimensional (4D) flow cardiovascular magnetic resonance, those for pediatric BAV patients have less frequently been reported, partly due to scarcity of data to define normal WSS range. To circumvent this challenge, this study aims to investigate if a recently proposed 4D flow-based hemodynamic measurement, abnormal flow directionality, is associated with aortic dilation in pediatric/young adult BAV patients.

Methods: 4D flow scans for BAV patients (< 20 years old) and age-matched controls were retrospectively enrolled. Static segmentation for the aorta and pulmonary arteries was obtained to quantify peak systolic hemodynamics and diameters in the proximal aorta. In addition to peak velocity, WSS, vorticity, helicity, and viscous energy loss, direction of aortic velocity and WSS in BAV patients were compared with that of control atlas using registration technique; angle differences of > 60 deg and > 120 deg were defined as moderately and severely abnormal, respectively. The association between the obtained metrics and normalized diameters (Z-scores) was evaluated at the sinotubular junction, mid-ascending aorta, and distal ascending aorta.

Results: Fifty-three BAV patients, including 18 with history of repaired aortic coarctation, and 17 controls were enrolled. Correlation between moderately abnormal velocity/WSS direction and aortic Z-scores was moderate to strong at the sinotubular junction and mid-ascending aorta ($R = 0.62–0.81$; $p < 0.001$) while conventional measurements exhibited weaker correlation ($|R| = 0.003–0.47$, $p = 0.009–0.99$) in all subdomains. Multivariable regression analysis found moderately abnormal velocity direction and existence of aortic regurgitation (only for isolated BAV group) were independently associated with mid-ascending aortic Z-scores.

Conclusion: Abnormal velocity and WSS directionality in the proximal aorta were strongly associated with aortic Z-scores in pediatric/young adult BAV patients.

Abbreviations: AAo, ascending aorta; BAV, bicuspid aortic valve; CMR, cardiovascular magnetic resonance; CoA, coarctation of aorta; PCMRA, phase-contrast magnetic resonance angiography; STJ, sinotubular junction; WSS, wall shear stress; 4D, four-dimensional; 3D, three-dimensional; IRB, institutional review board; RL, right-left; RN, right-noncoronary; LN, left-noncoronary

* Corresponding author.
E-mail addresses: takashi.fujiwara@cuanschutz.edu (T. Fujiwara), ladonna.malone@childrenscolorado.org (L.J. Malone), kathryn.chatfield@cuanschutz.edu (K.C. Chatfield), ajberthusen@gmail.com (A. Berthusen), brian.fonseca@childrenscolorado.org (B. Fonseca), lorna.browne@childrenscolorado.org (L.P. Browne), alex.barker@cuanschutz.edu (A.J. Barker).
[1] ORCID: 0000-0002-0565-0075.
[2] Present address: Kansas City University, 1750 Independence Ave, Kansas City, Missouri 64106, USA.

https://doi.org/10.1016/j.jocmr.2024.101102
Received 9 May 2024; Received in revised form 26 August 2024; Accepted 17 September 2024

1. Introduction

Bicuspid aortic valve (BAV) is one of the most common congenital heart defects, affecting 1%–2% of population and patients are more likely than the general population to have aortic dilation of the ascending aorta (AAo) [1]. Given the need to monitor the rate of aortic dilation and a higher risk of aortic dissection, lifelong imaging surveillance is recommended in adults who have aortic root, AAo, or both greater than 4.0 cm in diameter [2,3].

While the genetic origin of BAV remains a commonly considered factor associated with aortic dilation, hemodynamics have also been shown to play a crucial role in risk stratification of adult BAV patients [4]. In this context, the quantification of hemodynamics in the aorta has been conducted using time-resolved, three-dimensional phase-contrast cardiovascular magnetic resonance (4D flow CMR) imaging [5,6]. Specifically, recent 4D flow CMR studies have demonstrated strong evidence that abnormally elevated wall shear stress (WSS) magnitude is a promising biomarker predictive of aortic dilation and aortic wall tissue degradation in adult BAV patients [7–9].

Although aortic growth is more stable and the fatal events are less likely to occur compared to adults, aortic dilation is also present in many pediatric/young adult BAV patients [10,11]. In addition, comorbidities frequently seen in pediatric BAV patients, such as Turner syndrome or coarctation of the aorta (CoA), may affect underlying tissue biomechanics and thus aortic growth rates. Therefore, risk stratification to predict aortic dilation is also desired in pediatric cohort. For example, prior echocardiographic studies found aortic valve dysfunction (aortic valve stenosis and regurgitation) was associated with increased aortic growth in pediatric BAV patients [12,13]. However, these studies also mentioned those with normally functioning BAV had aortic dilation as well, suggesting the importance of routine monitoring regardless of valve dysfunction and the possible existence of other predictive biomarkers, such as abnormal WSS magnitude, as shown in the adult population. However, the wide variability in body size and limited amount of 4D flow CMR data available for healthy pediatric control data make it difficult to define normal physiologic WSS ranges as has been done in adults [7], and thus to identify abnormal WSS magnitude in pediatric population.

A recent adult study proposed the concept of abnormal WSS "directionality" to quantify disturbed flow in the aorta of BAV patients and found a good correlation between abnormal directionality and aortic diameter [14]. Given the dearth of normative data for the pediatric cohort due to the variation of WSS magnitude with age and size, we hypothesize this concept of "abnormal directionality" may be applicable to pediatric/young adult BAV patients. Thus, the aim of this study is to investigate if abnormal directionality of blood flow obtained from 4D flow CMR is associated with aortic dilation in pediatric patients with BAV.

2. Methods

2.1. Study cohort

With institutional review board (IRB) approval and waiver of consent for this retrospective study, 4D flow CMR exams of pediatric/young adult BAV patients (< 20 years old) were queried for inclusion in our study using a CMR database at Children's Hospital Colorado (Aurora, Colorado, USA). Fig. 1 shows the data collection process. Exclusionary criteria were (1) suboptimal 4D flow quality (e.g., severe aliasing that was uncorrectable in post-processing), (2) aortic valve surgery, (3) confirmed genetic defects, and (4) complex disease/circulation, such as Fontan. The final cohort was classified into two groups according to the existence of repaired CoA (BAV and CoA-BAV groups) [15,16]. Patients with concomitant valve anomalies (aortic stenosis and/or regurgitation) had their severity determined based on maximum velocity or regurgitant fraction at the aortic valve. This information was obtained from CMR (for regurgitant fraction) or echocardiography (for maximum velocity) reports, and the criteria for severity were similar to that used in a previous study [17]. For maximum velocity, when a same-day echo study was not available, the one closest to the CMR study date was chosen.

The CMR database was also queried for 4D flow scans of pediatric and young adult patients and volunteers (< 20 years old) to create an age-matched control atlas, which was used to determine normal flow characteristics (including directionality). Clinically indicated scans were included only when no cardiovascular/genetic abnormalities were

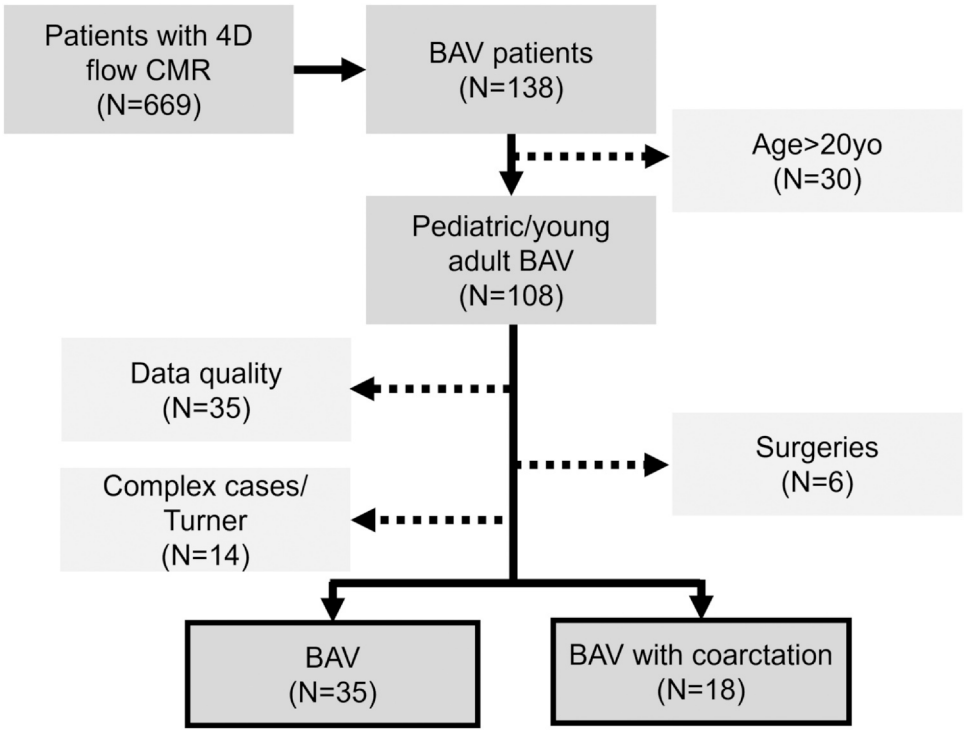

Fig. 1. Retrospective collection of 4D flow cardiovascular magnetic resonance (CMR) data. Bicuspid aortic valve (BAV) patients were identified from our 4D flow database (N = 669). Out of 108 pediatric/young adult BAV patients, those who underwent Fontan/Norwood/Ross surgeries (N = 6), data with quality issues, such as phase data with uncorrectable aliasing, were excluded (N = 35). After further exclusion of complex congenital heart defects and genetic defects (Turner syndrome, N = 12; hypoplastic left heart syndrome with patent ductus arteriosus, N = 1; double outlet right ventricle, N = 1), 35 BAV patients and 18 BAV patients with coarctation were finally included in this study. *4D* four dimensional

noted in the electronic health records and subjects were retrospectively included with IRB approval and waiver of consent. Healthy volunteer data were included via a prospective IRB-approved protocol and informed consent was obtained from the parent or legal guardian. Subject demographics were obtained from CMR reports and the CMR research database.

2.2. 4D flow CMR protocol

4D flow CMR data for patients and those with suspected cardiovascular anomalies were acquired as part of a clinically indicated scan protocol after administration of a gadolinium-based contrast agent. Patients were scanned on a Philips Ingenia 1.5T or 3T system (Philips Healthcare, Best, Netherland) using a standard 4D flow CMR protocol at our institution consisting of a retrospective electrocardiogram-gated and gradient recalled echo sequence with a sagittal-oblique orientation covering the whole heart and great vessels. Typical scan settings were: 3–4× SENSE (2× in phase, 1.5–2× in slice), flip angle = 14°, voxel size = 2.5 × 2.5 × 2.5 mm, velocity encoding = 150 cm/s, number of temporal phases = 18. When necessary, the settings were adjusted by the magnetic resonance imaging technologist to avoid artifacts (Table 2). All data were acquired during free breathing with a respiratory navigator placed on the lung-liver interface. Volunteers were scanned with the same conditions, without the use of contrast agents.

2.3. Post-processing and diameter/hemodynamic measurement on 4D flow CMR

The 4D flow data were pre-processed to remove phase offsets caused by eddy currents, background noise was masked, and aliased voxels were unwrapped using a custom MATLAB tool (MATLAB R2021a, MathWorks, Natick, Massachusetts) [18]. A three-dimensional (3D) phase-contrast magnetic resonance angiography (PCMRA) dataset was then computed from the magnitude and phase images (Fig. 2A). Based on the PCMRA, the aorta and pulmonary arteries were either labeled using a manual segmentation approach (for those who were already analyzed by human observers, i.e., T.F., 5 years of experience or A.B., with supervision by T.F.) or with a previously validated convolutional neural network [19,20]. Segmentation of all the subjects was visually inspected and corrected, if necessary, by an expert observer (T.F.) using 3D Slicer [21]. Segmentation of the aorta included the aortic valve, AAo, aortic arch, descending aorta as well as three branches at the arch, and was used to mask surrounding organs. Pulmonary arterial segmentation was used as a landmark to determine the aorta diameter measurement locations. The aortic centerline was computed from the aortic segmentation using the vascular modeling toolkit [22].

In addition to the acquired velocity data, peak systolic WSS, vorticity, normalized helicity density, and viscous energy loss were calculated using custom MATLAB tools [5,23–29]. To investigate the association between local hemodynamics and aortic diameter, diameter at the sinotubular junction (STJ, above the sinus of valsalva), mid-AAo (at the level of the right pulmonary artery), and distal-AAo (before the brachiocephalic artery) was measured based on the aortic segmentation and planes placed on the aortic centerline at 1 mm intervals (Fig. 2B) [30,31]. Planes at these three positions were manually chosen, and the diameters D were approximated as [32]:

$$D = 2\sqrt{\frac{A}{\pi}} \quad , \tag{1}$$

where A is the cross-sectional area of the vessel lumen. For diameter measurement, the aortic segmentation was up-sampled by a factor of 2 using linear interpolation. The measured diameter was normalized with Z-scores using echocardiography reference values and their regression equations [33]. To validate the PCMRA diameter measurement, the mid-AAo diameter measurements were compared to those in the CMR reports, which were obtained from cine steady-state free precession images orthogonally oriented to the AAo and contrast-enhanced magnetic resonance angiography (MRA) when cine steady-state free precession was unavailable.

2.4. Atlas-based flow directionality computation

The presence of abnormal directionality for velocity and WSS was measured according to the method proposed by van Ooij et al. (Fig. 3) [14]. This approach involved two steps: obtaining cohort-averaged normal directionality from controls (using the control atlas) and detecting abnormal directionality for individual BAV patients based on the control atlas. The averaged aortic geometry of the controls was first obtained by registration of the aortic segmentation with a degree of freedom (dof) of 3 (translation). Peak systolic velocity and WSS of each control were then mapped onto the averaged aortic geometry using affine registration (dof = 12) and trilinear interpolation was used to get cohort-averaged velocity and WSS vectors in the aorta. This control atlas was then registered to each patient's aortic geometry using affine transformation to map cohort-averaged velocity and WSS of controls onto patient's aorta. Finally, angle differences of velocity/WSS vectors between the control atlas and each patient were computed on a voxel-by-voxel basis. According to the previous study, angle differences larger than 60 deg but less than 12 deg were defined as moderately abnormal direction, while differences larger than 120 deg were defined as severely abnormal direction [14]. This led to a directionality map having three categorical values (normal, moderately, and severely abnormal directions) at each voxel over the aorta for each individual patient. A custom MATLAB tool was used for this analysis.

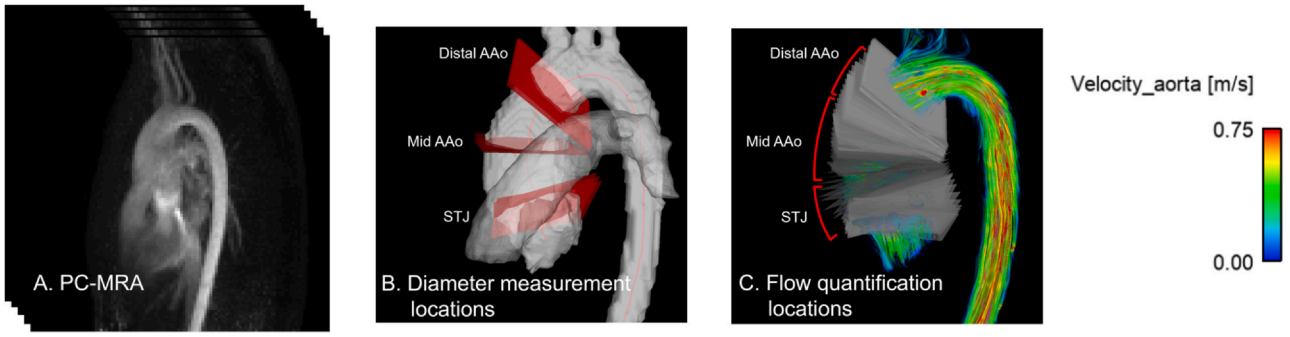

Fig. 2. Analysis strategy for diameter/flow measurements using 4D flow cardiac magnetic resonance. (A) A typical phase-contrast magnetic resonance angiography (PCMRA) image used for aortic segmentation. (B) After planes were placed along the aortic centerline, sinotubular junction (STJ), mid-ascending aorta (AAo), and distal-AAo were determined. (C) Based on the landmarks specified, planes were divided into three domains and averaged hemodynamics were used to investigate the correlation between hemodynamics and diameters. *4D* four dimensional

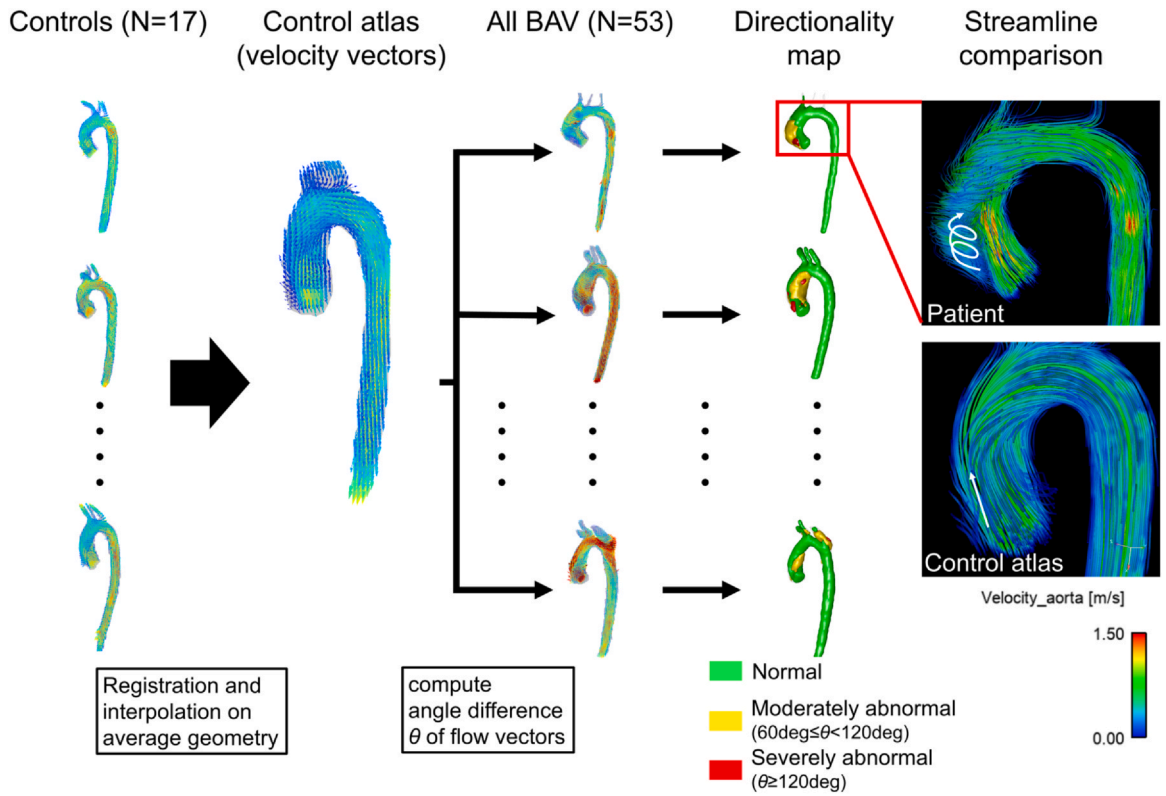

Fig. 3. Computation of abnormal flow directionality using control atlases. Aortic segmentations of controls were registered to determine averaged shape. Velocity and wall shear stress (WSS) vectors of the controls were mapped to the average geometry by affine registration and mean vectors were calculated at all the voxels of the aorta to create control atlas. The control atlas was then registered by affine registration to each bicuspid aortic valve (BAV) patient to calculate angle differences of the velocity/WSS vectors on patient's aortic geometry, with angle difference > 60 deg and > 120 deg defined as moderately and severely abnormal, respectively (yellow and red volumes in the directionality map). Examples showing the peak systolic streamlines illustrate the distinct difference in flow directions in the regions where abnormal directionality was detected

2.5. Subdomain analysis for the obtained hemodynamics

To investigate the association between local aortic diameter and the calculated aortic hemodynamics, the AAo and planes placed for diameter measurements were divided into three subdomains according to the three diameter measurement locations (Fig. 2C). The hemodynamic markers and directionality maps were interpolated onto the planes using trilinear interpolation. The in-plane hemodynamic markers and directionality maps were then averaged at the aortic subdomains to investigate their correlation to the local aortic Z-scores. Since directionality maps have categorical values, the moderately and severely abnormal directions were evaluated separately; the "occurrence" of moderately/severely abnormal directionality ranging from 0 (no abnormally directed vectors in the plane) to 1 (abnormal at all the elements in the plane) was computed for moderately/severely abnormal directions.

2.6. Statistical analysis

A Shapiro-Wilk test was used to check normality. Results are shown by means ± standard deviations or medians [interquartile ranges] depending on the normality of the data. A one-way analysis of variance or Kruskal-Wallis test was used with Bonferroni correction for comparison across all the cohorts. An unpaired t-test or Wilcoxon rank-sum test was used for comparison between BAV and CoA-BAV cohorts and between different valve phenotypes (right-left coronary cusp fusion [RL]- and right-noncoronary cusp fusion [RN]-fusion types). Pearson correlation and Bland-Altman analysis were used for comparison of diameters measured from 4D flow and those reported in CMR reports. Pearson correlation analysis was also employed to investigate the association between aortic Z-score and all the hemodynamic metrics obtained and was determined to be strong, moderate, or weak when the correlation coefficients were $|r| \geq 0.7$, $0.4 \leq |r| < 0.7$, and $0 \leq |r| < 0.4$, respectively. A multivariable linear regression with backward elimination was conducted using hemodynamic markers significantly correlating with AAo Z-scores as independent variables. Previously reported predictors for aortic dilation (existence of aortic stenosis or regurgitation and AAo peak velocity [12,13,16]) were also included and multicollinearity was checked. $p < 0.05$ was considered statistically significant. MATLAB R2021a and R 4.3.1 were used for statistical analysis.

3. Results

3.1. Subject demographics

Out of 108 potentially eligible pediatric/young adult patients with BAV, 55 patients were excluded (35 cases with uncorrectable aliasing in the AAo, 6 patients status post aortic valve surgeries, 14 complex cases such as patent ductus arteriosus, double outlet right ventricles, Turner syndrome; Fig. 1). Thus, 35 BAV and 18 CoA-BAV were included for analysis. Tables 1 and 2 summarize subject demographics and scan parameters. Mean ages were 15.0 ± 3.5, 15.4 ± 2.6, and 13.6 ± 3.2 years old for BAV, CoA-BAV, and control groups, respectively ($p = 0.20$). Right-left coronary, right-noncoronary, and left-noncoronary cusp fusions were seen in 60% (21/35), 26% (9/35), and 3% (1/35) of BAV, and 83% (15/18), 6% (1/18), and 0% (0/18) of CoA-BAV groups. Unicuspid aortic valve was reported in 11% (4/35) of the cases for both groups. Aortic stenosis was seen in 43% (15/35) of BAV and 28% (5/18) of CoA-BAV, whereas aortic regurgitation was

Table 1
Subject demographics.

	Controls (N = 17)	BAV (N = 35)	CoA-BAV (N = 18)	p
Female (%)	8 (47)	9 (26)	4 (22)	
Age at scan (y)	13.6 ± 3.2	15.0 ± 3.5	15.4 ± 2.6	0.20
Height (m)	1.57 ± 0.15	1.57 ± 0.21	1.67 ± 0.14	0.20
Weight (kg)	56.0 ± 22.0	52.0 ± 19.1	64.1 ± 21.5	0.14
BSA (m^2)	1.5 ± 0.4	1.5 ± 0.4	1.7 ± 0.3	0.19
Valve phenotype N (RL/RN/LN/unicuspid)	-	21/9/1/4	15/1/0/2	-
Aortic stenosis N (%)	-	15 (43)	5 (28)	-
Mild	-	9 (26)	3 (17)	-
Moderate	-	1 (3)	2 (11)	-
Severe	-	2 (6)	0 (0)	-
Aortic regurgitation N (%)	-	15 (43)	2 (11)	-
Mild	-	13 (37)	2 (11)	-
Moderate	-	2 (6)	0 (0)	-
Severe	-	0 (0)	0 (0)	-
Aortic Z-scores (measured on PCMRA)				
STJ	−0.8 ± 1.1	1.5 ± 1.4	0.5 ± 1.4	< **0.001**
Mid-AAo	0.8 ± 1.0	3.5 ± 1.5	2.3 ± 1.2	< **0.001**
Distal-AAo	0.7 ± 1.5	2.1 ± 1.4	0.8 ± 1.3	< **0.001**

BAV bicuspid aortic valve, *CoA* coarctation, *BSA* body surface area, *RL* right-left coronary cusp fusion, *RN* right-noncoronary cusp fusion, *LN* left-noncoronary cusp fusion, *PCMRA* phase-contrast magnetic resonance angiography, *STJ* sinotubular junction, *AAo* ascending aorta
Data are numbers (%) of cases or mean ± standard deviation. Statistical significance is shown by bold numbers

present in 43% (15/35) and 11% (2/18), respectively. Out of 18 repaired coarctation patients, 7 had catheter intervention and the others had surgery as the primary procedure. Three patients had stents at the time of exams. Four patients had subsequent procedures for recurrent or residual narrowing. One patient had significant residual coarctation at the time of the scan, which was confirmed by phase-contrast analysis of collateral flow and measurements. The mid-AAo diameter was not available for one patient. The diameter Z-scores were significantly different between control, BAV, and CoA-BAV groups except that no significant difference was found for distal-AAo Z-scores between control and CoA-BAV groups (Tables 1 and S1). Diameters measured using 4D flow CMR exhibited good agreement with those reported in the CMR radiologist reports as assessed by correlation ($R = 0.94$, $p < 0.001$), with a bias and limits of agreement of -2.3 ± 4.9 mm for 4D flow CMR (Fig. S1).

3.2. Hemodynamics in the ascending aorta

Post-processing and flow analysis was successfully conducted for all the patients and volunteers. Aliasing was found for 19 BAV and 11 CoA-BAV patients. Of them, 11 BAV and 3 CoA-BAV patients had uncorrectable residual aliasing in the focal region immediately distal to the aortic valve (i.e., in the vena contracta region) and hence these patients were only included using the mid- and distal-AAo analyses (omitting the aortic root region). Deep learning segmentation was employed for 17 subjects (3 controls, 10 BAV, and 4 CoA-BAV patients). A comparison of the hemodynamic markers between the BAV and CoA-BAV groups is shown in Table 3. Severely abnormal direction of WSS at the distal-AAo was not seen for 54% (19/35) and 83% (15/18) of BAV and CoA-BAV and was removed from the results (Table S2). Significantly higher mean velocity was found at distal-AAo in the CoA-BAV group. CoA-BAV patients also had significantly larger normalized helicity density at the mid-AAo and the distal-AAo. At the mid-AAo, severely abnormal direction was more often seen in the BAV group for both velocity and WSS. Moderately abnormal direction of velocity was more seen in the BAV group at the distal-AAo. Significant differences were also detected in severely abnormal direction of velocity at the distal-AAo, but the median values were low (< 0.01) in both groups. Subgroup analysis based on valve fusion types found no significant differences in any hemodynamic parameters between RN- and RL-fusion types, except that WSS and normalized helicity density were significantly larger and smaller in the RL-fusion group, respectively, at the STJ (Table S3).

3.3. Correlation between aortic hemodynamics and diameter

Correlations between hemodynamics in the AAo and diameter Z-scores are presented in Table 4. In the BAV group, no significant correlations were found for WSS at all levels of the AAo. Similarly, other conventional hemodynamic markers exhibited non-significant, weak correlation, except that normalized helicity density showed significant, moderate correlation with mid-AAo Z-scores. Conversely, moderately abnormal directions of velocity and WSS had moderate to strong positive correlations with the Z-scores at the STJ and mid-AAo. Significant

Table 2
Typical scan settings.

	Controls	BAV	CoA-BAV
Field strength (T) (3T/1.5T)	13/4	19/16	11/7
Echo time (ms)	2.4		
Repetition time (ms)	4.1		
Flip angle (deg)	7	7/14	
Velocity encoding (cm/s)	150	150–350	
Reconstruction temporal resolution (ms)	49	50	54
Voxel size (mm^3)	2.3 × 2.3 × 2.5	2.3 × 2.3 × 2.5	2.4 × 2.4 × 2.5
Acquisition matrix	100 × 100 × 44	112 × 112 × 45	128 × 128 × 50
Field of view (mm^3)	230 × 230 × 110	258 × 258 × 113	307 × 307 × 125
Acquisition time (min)	5:05	4:48	5:49

BAV bicuspid aortic valve, *CoA* aortic coarctation
Data are numbers of cases or representative numbers for each parameter.

Table 3
Hemodynamic metrics in the ascending aorta between groups.

	STJ			Mid-AAo			Distal-AAo		
	BAV (N = 24)	CoA-BAV (N = 15)	p	BAV (N = 35)	CoA-BAV (N = 18)	p	BAV (N = 35)	CoA-BAV (N = 18)	p
Velocity (m/s)	0.32 ± 0.08	0.35 ± 0.08	0.37	0.34 ± 0.08	0.39 ± 0.08	0.06	0.34 ± 0.10	0.42 ± 0.08	**0.004**
Peak velocity (m/s)	1.35 [1.15–1.50]	1.60 [1.30–1.90]	0.13	1.40 [1.13–1.78]	1.55 [1.2–1.8]	0.54	1.20 [1.10–1.58]	1.40 [1.20–1.50]	0.20
WSS (Pa)	0.95 ± 0.31	1.02 ± 0.32	0.53	1.27 ± 0.31	1.35 ± 0.37	0.43	1.39 ± 0.36	1.54 ± 0.30	0.15
Vorticity (1/s)	65 [53–76]	66 [59–76]	0.54	66 [56–75]	69 [59–79]	0.38	60 [49–79]	73 [68–88]	0.06
Normalized helicity (-)	0.02 ± 0.06	0.04 ± 0.06	0.35	0.05 ± 0.10	0.12 ± 0.06	**0.02**	0.05 ± 0.11	0.14 ± 0.04	**0.003**
Viscous energy loss (μW)	0.3 [0.20–0.51]	0.42 [0.27–0.61]	0.21	0.23 [0.16– 0.35]	0.32 [0.18–0.41]	0.29	0.19 [0.13–0.39]	0.08 [0–0.15]	0.06
Velocity direction (> 60 deg, < 120 deg)	0.10 [0.07–0.16]	0.09 [0.07–0.14]	0.56	0.23 [0.08–0.27]	0.09 [0.02–0.17]	0.07	0.10 [0.02–0.19]	0.01 [0.002–0.08]	**0.02**
Velocity direction (> 120 deg)	0.04 [0.01–0.08]	0.02 [0.01–0.04]	0.15	0.02 [0.002–0.05]	0.004 [0–0.008]	**0.02**	0.003 [0–0.04]	0 [0–0.001]	**0.02**
WSS direction (> 60 deg, < 120 deg)	0.24 [0.12–0.40]	0.29 [0.15–0.35]	0.76	0.37 [0.18–0.50]	0.27 [0.09–0.38]	0.11	0.22 [0.08–0.29]	0.03 [0–0.22]	0.06
WSS direction (> 120 deg)	0.10 [0.06–0.27]	0.09 [0.05–0.20]	0.77	0.03 [0–0.08]	0.001 [0–0.008]	**0.048**	-	-	-

STJ sinotubular junction, *AAo* ascending aorta, *BAV* bicuspid aortic valve, *CoA* aortic coarctation, *WSS* wall shear stress
Data are shown by means ± standard deviation or medians [interquartile range]. Statistical significance is shown by bold numbers

but weak to moderate correlations were also found for the distal-AAo. Severely abnormal direction of velocity had weak to moderate correlation at the STJ and mid-AAo.

Similar results were found in the CoA-BAV group, showing moderate to strong positive correlations for moderately abnormal directionality of velocity/WSS at the STJ and mid-AAo. However, severely abnormal direction showed no significant correlations. Conventional markers had non-significant, weak to moderate correlations with Z-scores, except for peak velocities at the mid-AAo.

Fig. 4 shows correlation plots between diameter Z-scores and WSS direction/magnitude at the mid-AAo for the BAV subgroup. No apparent relationship was detected between WSS magnitude and AAo Z-scores. WSS visualization for the three cases with different levels of Z-scores also confirmed WSS magnitude was not necessarily associated with AAo Z-scores. On the other hand, directionality of WSS exhibited a positive correlation. The streamline visualization in Fig. 4 demonstrates a transition from normal to abnormal flow direction as Z-score increases.

Given the correlation analysis, moderately and severely abnormal velocity/WSS direction as well as normalized helicity density were included in the multivariable linear regression analysis for BAV group while only moderately abnormal velocity/WSS direction was included for the CoA-BAV group (Table 5). Strong multicollinearity was seen between moderately abnormal velocity and WSS directions (variance inflation factor > 5) and hence WSS and velocity, which had a weaker correlation, were removed from independent variables of BAV and CoA-BAV groups, respectively. Mid-AAo Z-scores were independently associated with the existence of aortic regurgitation ($p = 0.04$) and moderately abnormal velocity direction ($p < 0.001$) in BAV patients and with moderately abnormal WSS direction ($p < 0.001$) for CoA-BAV patients.

4. Discussion

Given the difficulty of obtaining “normal” physiologic WSS magnitude values across a wide range of ages, and thus difficulty in identifying when the hemodynamic forces on the aorta wall are “abnormal,” this effort follows a method similar to van Ooij et al. to identify abnormal directionality of hemodynamic forces in a pediatric population [14]. This study demonstrated abnormal directionality of velocity and WSS was strongly correlated with proximal aortic Z-scores while conventional hemodynamic markers presented weaker correlation. In addition, moderately abnormal velocity/WSS direction and aortic regurgitation were independently associated with mid-AAo Z-scores. These results imply that abnormally directed flow may be a promising marker to monitor aortic dilation in pediatric BAV patients in lieu of WSS magnitude values.

Aortic flow in BAV patients is characterized by eccentric blood flow in the aorta, which results in abnormal aortic WSS [1,6]. Therefore, in adults, valve-dependent abnormal flow and WSS have been investigated by 4D flow CMR and proposed as a factor triggering aortic dilation [5]. In particular, recent studies have found that abnormally elevated WSS values are a key factor in initiating aortic dilation in adult BAV patients. Guzzardi et al. and Bollache et al. used age-matched control atlases to identify abnormally elevated WSS magnitude locations in the aorta and found it was associated with abnormal biomechanics and aortic wall tissue degeneration [8,34]. A 5-year follow-up 4D flow study further demonstrated that the area of abnormally high WSS was also predictive of aortic enlargement [7]. These recent findings provide convincing evidence that abnormally hemodynamics can initiate wall tissue remodeling and subsequent aortic dilation.

Despite these novel findings in adult population, 4D flow studies in pediatric BAV patients are scarce. Allen et al. conducted a cross-sectional study for pediatric BAV patients, where peak velocity in the AAo was associated with AAo WSS magnitude but no statistically significant correlation was found between WSS magnitude and aortic Z-score, which is in line with our study [16]. Another longitudinal study with up to 3.4-year follow-up found AAo peak velocity was a predictor for aortic

Table 4
Correlation coefficients (R) between aortic Z-scores at three levels and corresponding hemodynamics.

BAV	STJ (N = 24)		Mid-AAo (N = 35)		Distal-AAo (N = 35)	
	R	p	R	p	R	p
Mean velocity	−0.003	0.99	0.05	0.78	0.24	0.17
Peak velocity	0.30	0.16	0.21	0.22	−0.005	0.98
WSS	0.19	0.37	0.22	0.20	0.14	0.43
Vorticity	−0.05	0.80	−0.08	0.64	0.25	0.14
Normalized helicity density	−0.21	0.32	**−0.44**	**0.009**	−0.02	0.89
Viscous energy loss	−0.06	0.80	0.07	0.68	−0.02	0.91
Abnormal velocity direction (moderate: > 60 deg, < 120 deg)	**0.77**	**< 0.001**	**0.81**	**< 0.001**	**0.38**	**0.02**
Abnormal velocity direction (severe: > 120 deg)	**0.57**	**0.004**	**0.37**	**0.03**	−0.11	0.54
Abnormal WSS direction (moderate: > 60 deg, < 120 deg)	**0.62**	**0.001**	**0.69**	**< 0.001**	**0.42**	**0.01**
Abnormal WSS direction (severe: > 120 deg)	0.40	**0.06**	**0.36**	**0.03**	-	-
CoA-BAV	**STJ (N = 15)**		**Mid-AAo (N = 18)**		**Distal-AAo (N = 18)**	
	R	p	R	p	R	p
Mean velocity	−0.15	0.60	0.06	0.82	−0.15	0.54
Peak velocity	0.26	0.35	**0.47**	0.048	0.43	0.08
WSS	0.01	0.97	0.26	0.29	−0.10	0.68
Vorticity	0.11	0.68	0.12	0.63	0.02	0.95
Normalized helicity density	0.12	0.68	−0.08	0.77	−0.03	0.91
Viscous energy loss	−0.06	0.83	−0.08	0.76	0.01	0.96
Abnormal velocity direction (moderate: > 60 deg, < 120 deg)	**0.79**	**< 0.001**	**0.73**	**< 0.001**	0.39	0.11
Abnormal velocity direction (severe: > 120 deg)	0.29	0.29	0.32	0.20	0.25	0.32
Abnormal WSS direction (moderate: > 60 deg, < 120 deg)	**0.69**	**0.005**	**0.77**	**< 0.001**	0.39	0.11
Abnormal WSS direction (severe: > 120 deg)	0.20	0.48	−0.12	0.62	-	-

BAV bicuspid aortic valve, *CoA* coarctation, *WSS* wall shear stress, *STJ* sinotubular junction, *AAo* ascending aorta
Note that 11 BAV patients and 3 CoA-BAV patients were removed from the analysis at the STJ domain due to localized severe aliasing at the aortic root. Statistical significances are shown in bold numbers

dilation [17]. However, abnormal WSS magnitude for aortic dilation, the most promising biomarker in adults, has not been investigated in pediatric BAV patients. This is likely attributed to the larger variability in body size in the pediatric population and difficulty in collecting healthy volunteer 4D flow scans in pediatrics; this makes it challenging to define normal range of WSS magnitude. This is important because the detection of "abnormal" WSS magnitude relies on identifying when WSS is outside of the 95% confidence interval for normal physiologic variation. For example, van Ooij et al. compared abnormal WSS magnitude maps obtained from age-matched and -unmatched atlases, concluding age-unmatched atlases make the estimation of abnormal WSS magnitude maps inaccurate due to variability of WSS with age and postulate that likely the resulting age-related growth in aortic dimensions is responsible for this inaccuracy [35]. This result underpins the importance of age- and size-matched controls in estimating normal and abnormal WSS magnitude, as well as a critical challenge in pediatrics considering the need for a large database of age- and size-matched healthy subjects. As such, the use of an atlas-based approach to detect abnormal velocity directionality has been proposed by van Ooij et al. to quantify abnormal flow such as vorticity and helicity [14]. In contrast to the magnitude of WSS and velocity, it is hypothesized that the directionality of the hemodynamic forces may be less dependent on aortic size in controls. In an adult BAV cohort, they demonstrated a correlation between the abnormal direction and aortic diameter. Furthermore, abnormal directionality may be associated with abnormal WSS magnitude because both are induced by a strong jet from the aortic valve. With these hypotheses in mind, we attempted to apply the approach to a pediatric BAV cohort and found strong correlation between abnormal direction of velocity and WSS and aortic Z-scores. We were not able to confirm direct correlation between abnormal WSS magnitude and directionality in this study because abnormal WSS magnitude is difficult to obtain in pediatrics as discussed previously. Nonetheless, abnormal WSS directionality could be a surrogate of abnormal WSS magnitude and hence a good hemodynamic marker for aortic dilation in pediatric BAV patients, where abnormal WSS magnitude is less likely to be available.

As this is a cross-sectional study, care must be taken in the interpretation of these results; it does not necessarily mean abnormal directionality is a predictor for aortic dilation. However, recent longitudinal 4D flow studies investigating the direction of WSS demonstrated promising results. Minderhoud et al. used 4D flow CMR of adult BAV patients to clarify WSS angle (angle deviation from the aortic axis) was an independent predictor for aortic dilation, with implying a potential role of the magnitude of WSS as well [41]. Guala et al. focused on local hemodynamics and regional aortic growth and showed an association between circumferential WSS and aortic growth rate [36]. Their findings are in accordance with our results and do not contradict our hypothesis that abnormal WSS magnitude is a key trigger for aortic dilation and associated with abnormal direction of flow.

As already discussed, abnormal directionality was recently introduced to quantify helical and vortical flow [14]. In the prior study, a moderate correlation was found between severely abnormal flow directionality and vortex scoring conducted by human observers, as well as a moderate correlation between abnormal flow directionality and normalized helicity density. In our study, we found a stronger correlation between moderately abnormal flow directionality and aortic Z-scores than severely abnormal flow directionality. This may indicate that helical features of the ascending aortic flow are more associated with eccentric post-valvular flow features, which have been associated with aortic wall degeneration and hence aortic dilation [8,34,37].

Previous studies have found that the aortic growth rate in CoA-BAV patients is slower than those with isolated BAV, and aortic diameter is smaller in patients with CoA [14,38,39], which was also observed in our study. Nonetheless, Blais et al. have found unrepaired CoA is associated with progressive aortic growth, suggesting the importance of understanding hemodynamics in patients with BAV and CoA [13]. The strong

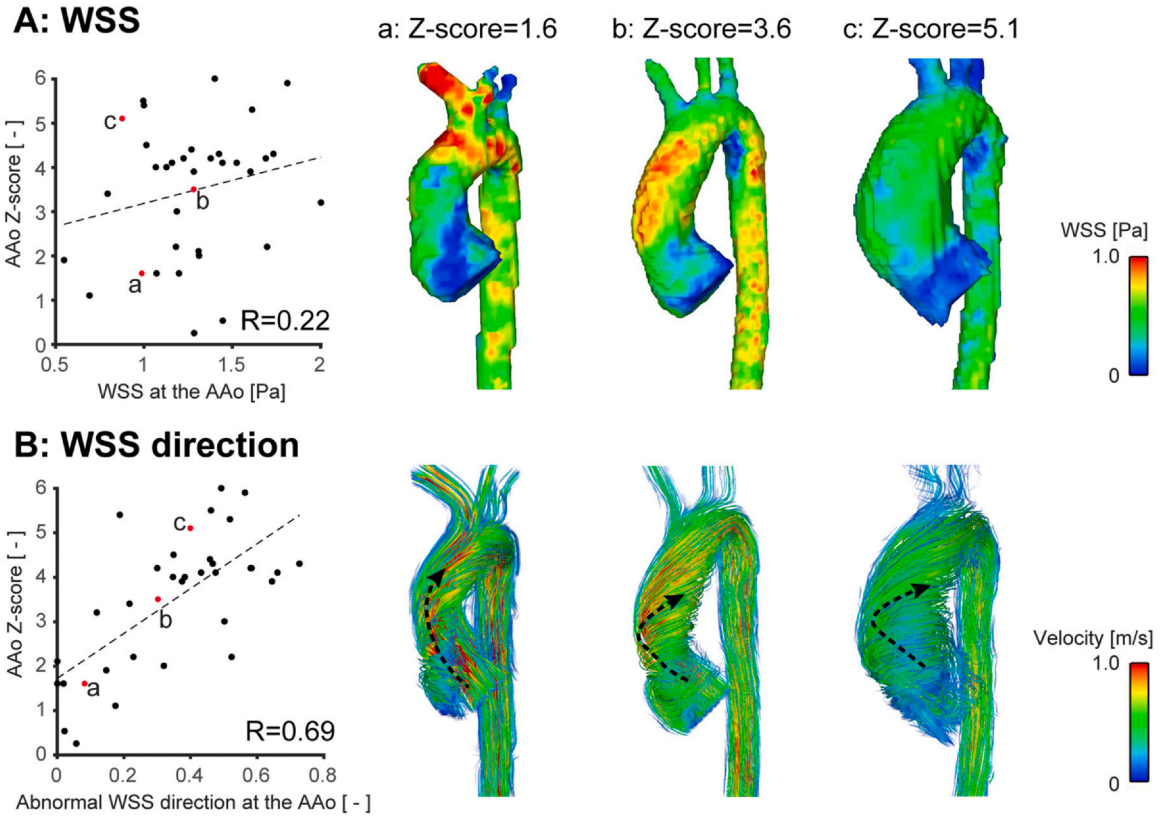

Fig. 4. Correlation plots between mid-ascending aortic (AAo) diameter Z-scores and wall shear stress (WSS) (A: WSS magnitude, B: moderately abnormal WSS direction) for the BAV subgroup. Peak systolic WSS magnitude and streamlines in the aorta are shown for three cases with different levels of Z-scores (a-c, red dots). Representative flow/WSS directions at the AAo were illustrated by black dotted arrows. As the aortic Z-score increases, direction of AAo flow becomes more abnormal due to vortical and/or helical flow while WSS magnitude varies independent of the aortic Z-score

Table 5
Multivariable regression analysis for mid-ascending aortic Z-score.

	Coefficient	Standard error	p
BAV			
Existence of aortic stenosis	-	-	-
Existence of aortic regurgitation	0.71	0.33	**0.04**
Peak velocity	−0.48	0.28	0.10
Normalized helicity density	-	-	-
Abnormal velocity direction (moderate)	11.40	1.47	< **0.001**
Abnormal velocity direction (severe)	-	-	-
Abnormal WSS direction (severe)	-	-	-
CoA-BAV			
Existence of aortic stenosis	-	-	-
Existence of aortic regurgitation	-	-	-
Peak velocity	-	-	-
Abnormal WSS direction (moderate)	4.65	0.97	< **0.001**

BAV bicuspid aortic valve, *CoA* coarctation
Moderately abnormal wall shear stress (WSS) and velocity directions were excluded from independent variables for BAV and CoA-BAV groups, respectively, as they exhibited multicollinearity with moderately abnormal velocity/WSS directions. Statistical significance is shown by bold numbers

correlation between the aortic Z-scores and flow directionality we found implies the concept of flow directionality may help capture the key hemodynamic features in CoA-BAV patients, but a dedicated study investigating how repaired and unrepaired CoA impact hemodynamics in the aorta, including flow directionality, is necessary in this cohort.

5. Limitations

One limitation of this study is a selection bias due to retrospective nature of this study. For example, most of those with moderate or severe aortic stenosis were excluded due to severe velocity aliasing covering the majority of the AAo region. This is probably the reason why aortic stenosis, a previously reported predictor, was not associated with aortic Z-score in our study [12,13]. To mitigate this bias as much as possible, we included patients with aortic stenosis when flow at the mid- and distal-AAo was measurable. Additional limitations include the limited number of controls available for creating atlases (N = 17). As mentioned previously, this is a common challenge with pediatric studies in which it is difficult to capture large numbers of age- and size-matched healthy controls. Volunteers were scanned without the administration of contrast agent. While this results in lower signal than the patients who receive contrast, acceptable image quality can be

achieved without contrast administration [40]. Additionally, it is not likely that the "normal direction" vectors used to determine abnormal directionality are grossly affected. Aortic diameters were obtained from PCMRA. The regression analysis in our study found a reasonable agreement between PCMRA and clinically reported diameters and a previous study demonstrated good agreement between PCMRA and contrast-enhanced MRA [32]. However, in this study, the Bland-Altman plot shows some underestimation between PCMRA and clinically reported diameters which need to be taken into consideration. Similar to the characterization performed in the adult population from the Garcia et al. study, future studies of the performance of image quality PCMRA-based diameter are needed in pediatric populations. Last, although subgroup comparison between different valve phenotypes was conducted, there was heterogeneity in the number of subjects (RL-fusion: 68% (36/53), RN-fusion: 19% (10/53)). Effects of valve phenotype on hemodynamics, including abnormal directionality, should also be considered in future studies with sufficient number of subjects for both fusion types.

6. Conclusion

In conclusion, this study found that an abnormal direction of velocity and WSS in the aorta was associated with AAo Z-scores in pediatric/young adult BAV patients, suggesting abnormal directionality is a promising hemodynamic parameter to research the potential role of hemodynamics in the development of pediatric aortopathy.

Funding

Research reported in this publication was supported by the National Heart, Lung, and Blood Institute of the National Institutes of Health under Award Number R01HL133504 (principal investigator: Alex J. Barker) and American Heart Association Grant #23POSTCHF1025444 (principal investigator: Takashi Fujiwara).

Author contributions

Takashi Fujiwara: Writing—original draft, Software, Methodology, Investigation, Formal analysis, Conceptualization. **LaDonna J. Malone:** Writing—review and editing, Resources. **Kathryn C. Chatfield:** Writing—review and editing. **Alex Berthusen:** Writing—review and editing, Investigation, Data curation. **Brian Fonseca:** Writing—review and editing. **Lorna P. Browne:** Writing—review and editing, Supervision, Resources. **Alex J. Barker:** Writing—review and editing, Supervision, Conceptualization.

Declaration of competing interests

The authors declare that they have no known competing financial interests or personal relationships that could have appeared to influence the work reported in this paper.

Acknowledgements

Not applicable.

Appendix A. Supporting information

Supplementary data associated with this article can be found in the online version at doi:10.1016/j.jocmr.2024.101102.

References

[1] Verma S, Siu SC. Aortic dilatation in patients with bicuspid aortic valve. N Engl J Med 2014;370:1920–9. https://doi.org/10.1056/NEJMra1207059.
[2] Ward C. Clinical significance of the bicuspid aortic valve. Heart 2000;83:81–5. https://doi.org/10.1136/heart.83.1.81.
[3] Isselbacher EM, Preventza O, Hamilton Black III J, Augoustides JG, Beck AW, Bolen MA, et al. 2022 ACC/AHA guideline for the diagnosis and management of aortic disease: a report of the American Heart Association/American College of Cardiology joint committee on clinical practice guidelines. Circulation 2022;146:e334–482. https://doi.org/10.1161/CIR.0000000000001106.
[4] Bissell MM, Hess AT, Biasiolli L, Glaze SJ, Loudon M, Pitcher A, et al. Aortic dilation in bicuspid aortic valve disease: flow pattern is a major contributor and differs with valve fusion type. Circ Cardiovasc Imaging 2013;6:499–507. https://doi.org/10.1161/CIRCIMAGING.113.000528.
[5] Barker AJ, Markl M, Burk J, Lorenz R, Bock J, Bauer S, et al. Bicuspid aortic valve is associated with altered wall shear stress in the ascending aorta. Circ Cardiovasc Imaging 2012;5:457–66. https://doi.org/10.1161/CIRCIMAGING.112.973370.
[6] Hope MD, Hope TA, Crook SE, Ordovas KG, Urbania TH, Alley MT, et al. 4D flow CMR in assessment of valve-related ascending aortic disease. JACC Cardiovasc Imaging 2011;4(7):781. https://doi.org/10.1016/j.jcmg.2011.05.004.
[7] Soulat G, Scott MB, Allen BD, Avery R, Bonow RO, Malaisrie SC, et al. Association of regional wall shear stress and progressive ascending aorta dilation in bicuspid aortic valve. JACC Cardiovasc Imaging 2022;15:33–42. https://doi.org/10.1016/j.jcmg.2021.06.020.
[8] Guzzardi DG, Barker AJ, van Ooij P, Malaisrie SC, Puthumana JJ, Belke DD, et al. Valve-related hemodynamics mediate human bicuspid aortopathy: insights from wall shear stress mapping. J Am Coll Cardiol 2015;66:892–900. https://doi.org/10.1016/j.jacc.2015.06.1310.
[9] Nightingale M, Scott MB, Sigaeva T, Guzzardi DG, Garcia J, Malaisrie C, et al. Magnetic resonance imaging-based hemodynamic wall shear stress alters aortic wall tissue biomechanics in bicuspid aortic valve patients. J Thorac Cardiovasc Surg 2023;168:465–76. https://doi.org/10.1016/j.jtcvs.2022.12.021. e5.
[10] Spaziani G, Ballo P, Favilli S, Fibbi V, Buonincontri L, Pollini I, et al. Clinical outcome, valve dysfunction, and progressive aortic dilation in a pediatric population with isolated bicuspid aortic valve. Pediatr Cardiol 2014;35:803–9. https://doi.org/10.1007/s00246-013-0856-4.
[11] Yamauchi MSW, Puchalski MD, Weng HT, Pinto NM, Etheridge SP, Presson AP, et al. Disease progression and variation in clinical practice for isolated bicuspid aortic valve in children. Congenit Heart Dis 2018;13:432–9. https://doi.org/10.1111/chd.12591.
[12] Grattan M, Prince A, Rumman RK, Morgan C, Petrovic M, Hauck A, et al. Predictors of bicuspid aortic valve-associated aortopathy in childhood: a report from the MIBAVA consortium. Circ Cardiovasc Imaging 2020;13:e009717. https://doi.org/10.1161/CIRCIMAGING.119.009717.
[13] Blais S, Meloche-Dumas L, Fournier A, Dallaire F, Dahdah N. Long-term risk factors for dilatation of the proximal aorta in a large cohort of children with bicuspid aortic valve. Circ Cardiovasc Imaging 2020;13:e009675. https://doi.org/10.1161/CIRCIMAGING.119.009675.
[14] van Ooij P, Farag ES, Blanken CPS, Nederveen AJ, Groenink M, Planken RN, et al. Fully quantitative mapping of abnormal aortic velocity and wall shear stress direction in patients with bicuspid aortic valves and repaired coarctation using 4D flow cardiovascular magnetic resonance. J Cardiovasc Magn Reson 2021;23:9. https://doi.org/10.1186/s12968-020-00703-2.
[15] Ciotti GR, Vlahos AP, Silverman NH. Morphology and function of the bicuspid aortic valve with and without coarctation of the aorta in the young. Am J Cardiol 2006;98:1096–102. https://doi.org/10.1016/j.amjcard.2006.05.035.
[16] Allen BD, van Ooij P, Barker AJ, Carr M, Gabbour M, Schnell S, et al. Thoracic aorta 3D hemodynamics in pediatric and young adult patients with bicuspid aortic valve. J Magn Reson Imaging 2015;42:954–63. https://doi.org/10.1002/jmri.24847.
[17] Rose MJ, Rigsby CK, Berhane H, Bollache E, Jarvis K, Barker AJ, et al. 4-D flow MRI aortic 3-D hemodynamics and wall shear stress remain stable over short-term follow-up in pediatric and young adult patients with bicuspid aortic valve. Pediatr Radiol 2019;49:57–67. https://doi.org/10.1007/s00247-018-4257-y.
[18] Bock J, Kreher B, Hennig J, Markl M. Optimized pre-processing of time-resolved 2D and 3D phase contrast MRI data. Proc Int Soc Magn Reson Med 2007;15:3138.
[19] Fujiwara T, Berhane H, Scott MB, Englund EK, Schafer M, Fonseca B, et al. Segmentation of the aorta and pulmonary arteries based on 4D flow MRI in the pediatric setting using fully automated multi-site, multi-vendor, and multi-label dense U-Net. J Magn Reson Imaging 2022;55:1666–80. https://doi.org/10.1002/jmri.27995.
[20] Berhane H, Scott M, Elbaz M, Jarvis K, McCarthy P, Carr J, et al. Fully automated 3D aortic segmentation of 4D flow MRI for hemodynamic analysis using deep learning. Magn Reson Med 2020;84:2204–18. https://doi.org/10.1002/mrm.28257.
[21] Fedorov A, Beichel R, Kalpathy-Cramer J, Finet J, Fillion-Robin JC, Pujol S, et al. 3D Slicer as an image computing platform for the quantitative imaging network. Magn Reson Imaging 2012;30:1323–41. https://doi.org/10.1016/j.mri.2012.05.001.
[22] Antiga L, Piccinelli M, Botti L, Ene-Iordache B, Remuzzi A, Steinman DA. An image-based modeling framework for patient-specific computational hemodynamics. Med Biol Eng Comput 2008;46:1097–112. https://doi.org/10.1007/s11517-008-0420-1.
[23] Frydrychowicz A, Markl M, Hirtler D, Harloff A, Schlensak C, Geiger J, et al. Aortic hemodynamics in patient with and without repair of aortic coarctation. Invest Radiol 2011;46:317–25. https://doi.org/10.1097/RLI.0b013e3182034fc2.
[24] Hirtler D, Garcia J, Barker AJ, Geiger J. Assessment of intracardiac flow and vorticity in the right heart of patients after repair of tetralogy of Fallot by flow-sensitive 4D MRI. Eur Radiol 2016;26:3598–607. https://doi.org/10.1007/s00330-015-4186-1.
[25] Garcia J, Barker AJ, Collins JD, Carr JC, Markl M. Volumetric quantification of absolute local normalized helicity in patients with bicuspid aortic valve and aortic dilatation. Magn Reson Med 2017;78:689–701. https://doi.org/10.1002/mrm.26387.

[26] Schafer M, Barker AJ, Jaggers J, Morgan GJ, Stone ML, Truong U, et al. Abnormal aortic flow conduction is associated with increased viscous energy loss in patients with repaired tetralogy of Fallot. Eur J Cardiothorac Surg 2020;57:588–95. https://doi.org/10.1093/ejcts/ezz246.
[27] van Ooij P, Potters WV, Nederveen AJ, Allen BD, Collins J, Carr J, et al. A methodology to detect abnormal relative wall shear stress on the full surface of the thoracic aorta using four-dimensional flow MRI. Magn Reson Med 2015;73:1216–27. https://doi.org/10.1002/mrm.25224.
[28] Barker AJ, van Ooij P, Bandi K, Garcia J, Albaghdadi M, McCarthy P, et al. Viscous energy loss in the presence of abnormal aortic flow. Magn Reson Med 2014;72:620–8. https://doi.org/10.1002/mrm.24962.
[29] Garcia J, Larose E, Pibarot P, Kadem L. On the evaluation of vorticity using cardiovascular magnetic resonance velocity measurements. J Biomech Eng 2013;135:124501. https://doi.org/10.1115/1.4025385.
[30] Borger MA, Fedak PWM, Stephens EH, Gleason TG, Girdauskas E, Ikonomidis JS, et al. The American Association for Thoracic Surgery consensus guidelines on bicuspid aortic valve-related aortopathy: full online-only version. J Thorac Cardiovasc Surg 2018;156:e41–74. https://doi.org/10.1016/j.jtcvs.2018.02.115.
[31] Jarvis K, Scott MB, Soulat G, Elbaz MSM, Barker AJ, Carr JC, et al. Aortic pulse wave velocity evaluated by 4D flow MRI across the adult lifespan. J Magn Reson Imaging 2022;56:464–73. https://doi.org/10.1002/jmri.28045.
[32] Garcia J, Barker AJ, Murphy I, Jarvis K, Schnell S, Collins JD, et al. Four-dimensional flow magnetic resonance imaging-based characterization of aortic morphometry and haemodynamics: impact of age, aortic diameter, and valve morphology. Eur Heart J Cardiovasc Imaging 2016;17:877–84. https://doi.org/10.1093/ehjci/jev228.
[33] Pettersen MD, Du W, Skeens ME, Humes RA. Regression equations for calculation of z scores of cardiac structures in a large cohort of healthy infants, children, and adolescents: an echocardiographic study. J Am Soc Echocardiogr 2008;21:922–34. https://doi.org/10.1016/j.echo.2008.02.006.
[34] Bollache E, Guzzardi DG, Sattari S, Olsen KE, Di Martino ES, Malaisrie SC, et al. Aortic valve-mediated wall shear stress is heterogeneous and predicts regional aortic elastic fiber thinning in bicuspid aortic valve-associated aortopathy. J Thorac Cardiovasc Surg 2018;156:2112–2120 e2. https://doi.org/10.1016/j.jtcvs.2018.05.095.
[35] van Ooij P, Garcia J, Potters WV, Malaisrie SC, Collins JD, Carr JC, et al. Age-related changes in aortic 3D blood flow velocities and wall shear stress: implications for the identification of altered hemodynamics in patients with aortic valve disease. J Magn Reson Imaging 2016;43:1239–49. https://doi.org/10.1002/jmri.25081.
[36] Guala A, Dux-Santoy L, Teixido-Tura G, Ruiz-Munoz A, Galian-Gay L, Servato ML, et al. Wall shear stress predicts aortic dilation in patients with bicuspid aortic valve. JACC Cardiovasc Imaging 2022;15:46–56. https://doi.org/10.1016/j.jcmg.2021.09.023.
[37] Mahadevia R, Barker AJ, Schnell S, Entezari P, Kansal P, Fedak PW, et al. Bicuspid aortic cusp fusion morphology alters aortic three-dimensional outflow patterns, wall shear stress, and expression of aortopathy. Circulation 2014;129:673–82. https://doi.org/10.1161/CIRCULATIONAHA.113.003026.
[38] Sophocleous F, Berlot B, Ordonez MV, Baquedano M, Milano EG, De Francesco V, et al. Determinants of aortic growth rate in patients with bicuspid aortic valve by cardiovascular magnetic resonance. Open Heart 2019;6:e001095. https://doi.org/10.1136/openhrt-2019-001095.
[39] Beaton AZ, Nguyen T, Lai WW, Chatterjee S, Ramaswamy P, Lytrivi ID, et al. Relation of coarctation of the aorta to the occurrence of ascending aortic dilation in children and young adults with bicuspid aortic valves. Am J Cardiol 2009;103:266–70. https://doi.org/10.1016/j.amjcard.2008.09.062.
[40] Bissell MM, Raimondi F, Ait Ali L, Allen BD, Barker AJ, Bolger A, et al. 4D Flow cardiovascular magnetic resonance consensus statement: 2023 update. J Cardiovasc Magn Reson 2023;25:40. https://doi.org/10.1186/s12968-023-00942-z.
[41] Minderhoud SCS, Roos-Hesselink JW, Chelu RG, Bons LR, van den Hoven AT, Korteland SA, et al. Wall shear stress angle is associated with aortic growth in bicuspid aortic valve patients. Eur Heart J Cardiovasc Imaging 2022;23:1680–9. https://doi.org/10.1093/ehjci/jeab290.